Molecular Crystals and Liquid Crystals
Publication details, including instructions for authors and subscription information:
http://www.tandfonline.com/loi/gmcl20

Improved Organic Thin Film Transistor Performance Utilizing a DH-α6T Submonolayer

Yusuke Fujinaka [a] , Rongbin Ye [b] , Koji Ohta [b] , Kazume Nishidate [b] & Mamoru Baba [b]

[a] Graduate School of Engineering , Iwate University , Morioka , Japan

[b] Faculty of Engineering , Iwate University , Morioka , Japan

Published online: 11 Sep 2013.

To cite this article: Yusuke Fujinaka , Rongbin Ye , Koji Ohta , Kazume Nishidate & Mamoru Baba (2013) Improved Organic Thin Film Transistor Performance Utilizing a DH-α6T Submonolayer, Molecular Crystals and Liquid Crystals, 580:1, 110-116, DOI: 10.1080/15421406.2013.808112

To link to this article: http://dx.doi.org/10.1080/15421406.2013.808112

Mol. Cryst. Liq. Cryst., Vol. 580: pp. 110–116, 2013

ISSN: 1542-1406 print/1563-5287 online
DOI: 10.1080/15421406.2013.808112

Taylor & Francis
Taylor & Francis Group

Improved Organic Thin Film Transistor Performance Utilizing a DH-α6T Submonolayer

YUSUKE FUJINAKA,[1] RONGBIN YE,[2,*] KOJI OHTA,[2] KAZUME NISHIDATE,[2] AND MAMORU BABA[2]

[1]Graduate School of Engineering, Iwate University, Morioka, Japan
[2]Faculty of Engineering, Iwate University, Morioka, Japan

In this paper, we have reported on improved titanyl phthalocyanine (TiOPc) thin film transistor (TFT) performance utilizing an α,α′-dihexylsexithiophene (DH-α6T) submonolayer. By the detailed XRD and AFM analysis, highly ordering α-TiOPc thin films could be deposited on SiO_2/Si substrates modified by a DH-α6T submonolayer. Organic TFT with a TiOPc/ DH-α6T bilayer as active layers realized high mobility of 2.45 × 10^{-1} cm^2 /V s, which is about 100 times greater than that of TiOPc single layer device.

Keywords Field-effect mobility; organic semiconductors; organic thin film transistors

1. Introduction

Metal phthalocyanines (MPcs) are organic dye materials, used in printing inks, as colorants for plastics and fibers, and their semiconducting properties are exploited for applications such as thin film transistors (TFTs), light emitting diodes, solar cells and gas sensors [1–15]. Titanyl phthalocyanine (TiOPc), one of non-planar phthalocyanines, has five polymorphs with different preparation and treatment procedures [8–15]. Specially, α-TiOPc presents a particularly efficient charge photogeneration and a strong optical absorption in the red and near-IR spectral regions and a very promising organic semiconductor with high mobility due to showing the pi-stacking structure with concave pair and convex pair with significant molecular overlaps and very short intermolecular distance [15]. Highly ordering α-TiOPc thin films could be deposited on Au or SiO_2/Si substrates modified by self-assembled monolayer at a high substrate temperature [15, 16].

M. A. Loi et al. have reported supramolecular organization in ultrathin films of α-sexithiophene (α6T) on silicon dioxide [17]. In submonolayer films of α6T, regions where the molecules stand on their long molecular axis coexist with regions where the molecules lie flat on the substrate. When the first monolayer is completed, all α6T molecules stand on the substrate, and the flat molecules detected in the submonolayer films are no longer present. End substitution of oligothiophenes by alkyl groups ensures highly organized films [18]. Therefore α,α′-dihexylsexithiophene (DH-α6T) is a more optimum material for supramolecular organization than α6T, pentacence and para-sexiphenyl (p-6P) [19–21]. On the other hand, it has been known that highly ordered films of MPCs can be fabricated on

*Address correspondence to Rongbin Ye, Faculty of Engineering, Iwate University, Morioka 020-8551, Japan. E-mail: ye@iwate-u.ac.jp

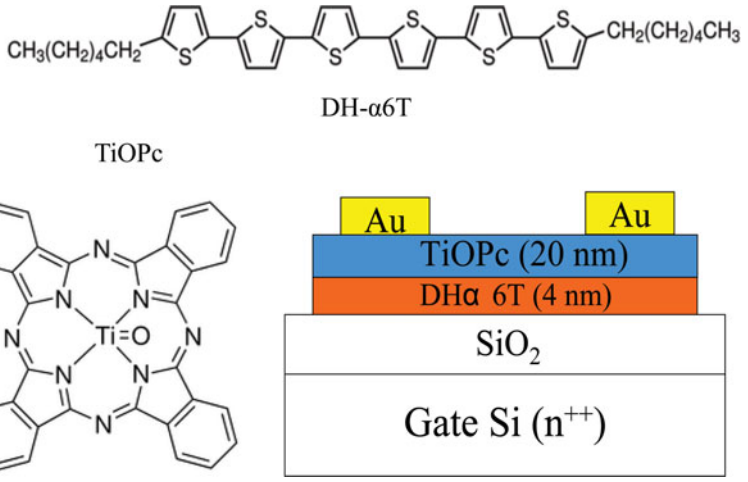

Figure 1. Chemical structure of TiOPc and DH-α6T, and schematic structure of organic TFTs.

p-6P submonolayer modified SiO_2/Si substrates by weak epitaxy growth, and the corresponding device performance is improved [22]. In this study, we report on improved TiOPc TFT performance utilizing DH-α6T submonolayer.

2. Experimental

Figure 1 shows the chemical structures of DH-α6T and TiOPc, and the schematic structure of organic TFT. Heavily n-doped Si substrate acts as the gate electrode with a 300 nm thermally grown SiO_2 layer ($C_i \sim 10$ nF/cm^2) as the gate dielectric. The sample of DH-α6T and TiOPc were purchased from Sigma Aldrich. DH-α6T thin film of approximately 4 nm thickness (first layer) and TiOPc thin film of approximately 20 nm thickness (second layer) were vacuum deposited from two deposition sources. During deposition, substrate temperature was set at 110°C under a base pressure of less than 1×10^{-3} Pa. The substrate temperature was controlled by a digital programming regulator (CHINO KP1000). Film thicknesses and growth rate were monitored by a thickness and growth rate monitor (ULVAC CRTM-6000). Finally, Au source and drain electrodes of 20 nm were vacuum deposited through a shadow mask with a channel with a channel width of 1 mm and length of 50 μm. The characteristics of OTFTs were measured using a two-channel voltage current source/monitor system (Advantest R6245) under ambient laboratory air condition.

The XRD analysis was performed on a diffractometer (Rint 2200V, RIGAKU Co., Ltd.) with graphite monochromatized CuK_α radiation ($\lambda = 1.54$ Å), operating in the Θ-2Θ mode. The morphology of the films was examined using AFM (Nanocute, Seiko Instruments Co., Ltd.), the cantilevers were used in the tapping mode with a length of 90 μm and a force constant of 0.12 N/m. The grain size (GS) were given by the AFM instrument for the individual scans (3 μm $\times$ 3 μm).

3. Results and Discussion

In Fig. 2(a), the typical XRD patterns of DH-α6T thin films of 10 nm with d_{001} spacing of 3.29 nm ($2\Theta = 2.68°$) was observed, and DH-α6T molecules are standing up with respect

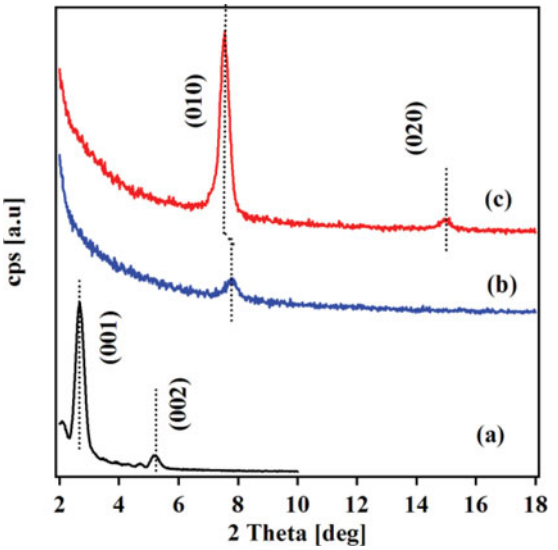

Figure 2. XRD patterns of (a) DH-α6T thin films of 10 nm, (b) a TiOPc single layer of 20 nm and (c) a 20 nm/4 nm of TiOPc/DH-α6T bilyer deposited on SiO_2/Si substrates at 110°C.

to substrate surface. The value of d_{001} is slightly smaller than that of DH-α6T thin films deposited on Si substrates [18]. Figure 2(b) shows XRD patterns of TiOPc thin films of 20 nm deposited on SiO_2/Si substrate at 110°C. Only a weak peak at $2\theta = 7.55°$ with $d_{010} =$ 1.14 nm was observed, which is assigned to α-phase. The XRD pattern of TiOPc films deposited on DH-α6T submonolyer modified SiO_2/Si substrates at 110°C was displayed in Fig. 2(c). An intense and sharp peak at 7.55° ($d_{010} = 1.17$ nm) due to the diffraction from (010) plane of α-phase was observed, which indicates highly ordered α-phase films with the (010) lattice plane parallel to the substrate, i.e., TiOPc molecules preferentially stood on substrates with an "edge-on" style orientation [16]. Moreover, the appearance of the second-order diffraction peak at 14.95° ($d_{020} = 0.592$ nm) further enhanced the high order of the vacuum deposited films. The above results suggested that TiOPc showed the weak epitaxy growth behavior, which inducted an ordered DH–α6T submonolayer to reduce the interaction between organic semiconductor molecules and the substrate, as similar to vanady-phthalocyanine deposited on p-6p submonolayer [22]. Hence, it was promising that high performance organic TFTs could be available based on the highly ordered vacuum deposited films with the "edge-on" molecular orientation because charge transport was along the pi-stacking direction [19].

Figure 3(a) gives the height AFM image of a DH-α6T submonolyer (~0.94 ML) deposited on SiO_2/Si substrate at 110°C and the nominal film thickness of is 4 nm. From the cross-sectional profile data corresponding to the black line in Fig. 3(a), the height of 1 ML is about 3.2 nm, which agrees with the above-stated XRD data. In Fig. 3(b), many small projections with GS of ca. 85 nm are observed. The TiOPc film deposited on DH-α6T submonolyer modified SiO_2/Si substrates at 110°C was consisted of lamellar crystals with GS of ca. 320 nm [Fig. 3 (c)], which were intimately connected with each other.

Figure 4 shows output characteristics of the TiOPc single layer and TiOPc/DH-α6T bilayer TFTs with various negative gate voltages. These devices typically work in p-channel accumulation mode. Compared with the TiOPc device, the saturated drain current of the

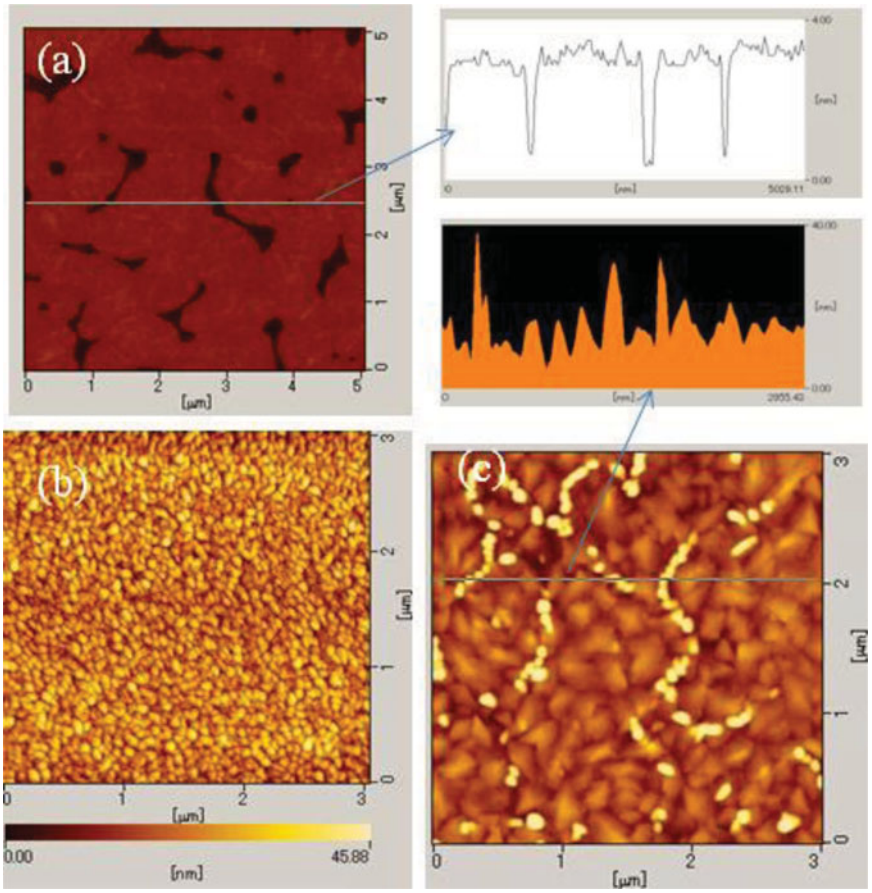

Figure 3. AFM images of (a) a DH-α6T submonolyer of 4 nm with cross-sectional profile data corresponding to the black line, (b) the TiOPc single layer of 20 nm and (c) the 20 nm/4 nm of TiOPc/DH-α6T bilayer with cross-sectional profile data corresponding to the black line (All thin films deposited on SiO_2/Si substrates at 110°C).

bilayer device at $V_D = V_G = -60$ V was enhanced up to over 190 times. Generally, the device performance of TFTs is evaluated with field-effect mobility (μ) and threshold voltage (V_T) extracted using the saturated drain current I_D vs. V_G relation [23]:

$$I_D = \left(\frac{W}{2L}\right) C_i \mu (V_G - V_T)^2, \tag{1}$$

where W, L and C_i are channel width, channel length and gate dielectric capacitance per unit area, respectively. From the transfer characteristics of the two devices with that of a DH-α6T submonolyer reference device (in Figure 5), mobilities and threshold voltages of these devices are obtained and listed in Table 1. The bilayer device shows high mobility that is about 100 times greater than that of the single layer device, which originated from highly ordering and increasing of grain size of TiOPc thin films deposited on a DH-α6T submonolayer.

Table 1. Summary of mobilities and threshold voltages for the DH-α6T submonolyer, the TiOPc single layer and the TiOPc/DH-α6T bilayer devices

Active layer	μ (cm^2/Vs)	V_T (V)
DH-α6T submonolyer	4.71×10^{-2}	−7.05
TiOPc single layer	2.52×10^{-3}	−13.95
DH-α6T/TiOPc bilayer	2.45×10^{-1}	−2.34

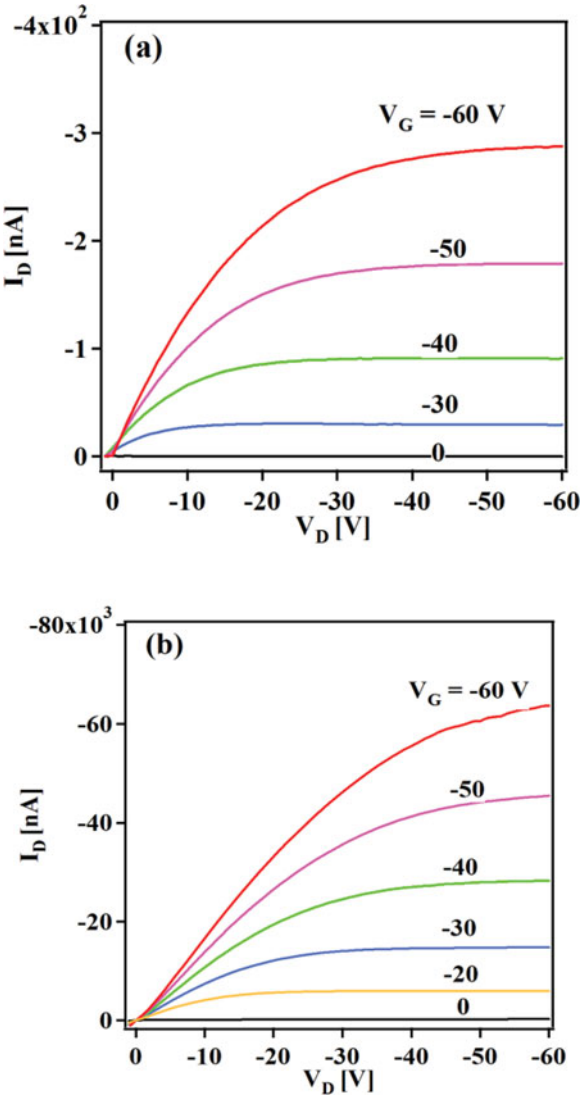

Figure 4. Output characteristics of (a) the TiOPc single layer of 20 nm and (b) the 20 nm/4 nm of TiOPc/DH-α6T bilayer TFTs.

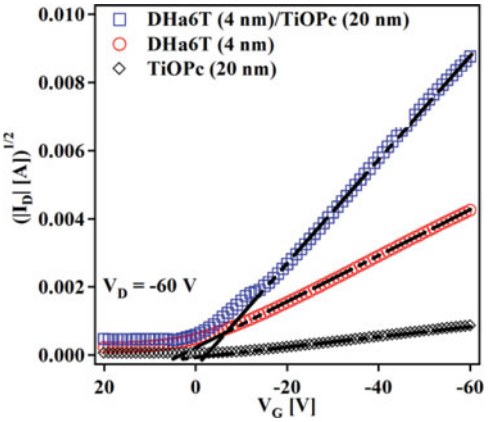

Figure 5. Transfer characteristics of the DH-α6T submonolyer, the TiOPc single layer, and the TiOPc/DH-α6T bilayer TFTs.

On the other hand, the mobility in an OTFT is generally gate bias dependent and can be estimated by considering the channel conductance [24],

$$g_{DS} = \frac{\partial I_D}{\partial V_G}, \tag{2}$$

measured at low V_D. In this case being $V_D \prec V_G$, g_{DS} can be expressed as followed:

$$g_{DS} = \frac{\partial I_D}{\partial V_D} \approx \frac{W}{L} C_i \mu (V_G - V_T). \tag{3}$$

In Fig. 6 the data for g_{DS} extracted from the output characteristics of Fig. 4 at $V_D = -5$V, are plotted as a function of V_G. The extracted mobilities are of 1.29×10^{-1} cm^2 /V s

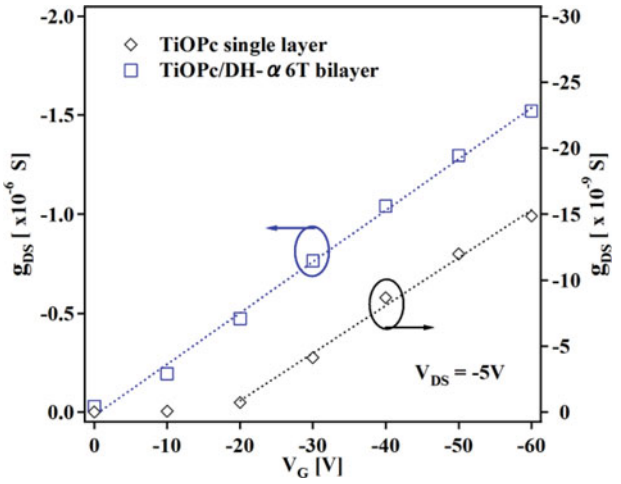

Figure 6. Channel conductance of the TiOPc single layer and TiOPc/DH-α6T bilayer TFTs plotted as a function of the gate bias.

and 1.81×10^{-3} cm^2/V s, respectively. Compared to the single layer device, the transport in the channel region of the bilayer device appears as not limited by the g_{DS}, since g_{DS}shows a quite good linear dependence from V_G. The$g_{DS}$of the bilayer layer device is about 100-fold bigger than that of the single layer device at of V_G < -20 V. Therefore, bigger g_{DS} also attributed to the increasing of mobility.

4. Conclusions

We have investigated improved TiOPc TFT performance utilizing a DH-α6T submonolayer. By the detailed XRD and AFM analysis, highly ordering α-TiOPc thin films with GS of ca. 320 nm could be deposited on SiO_2/Si substrates modified by a DH-α6T submonolayer. The TiOPc/DH-α6T bilayer device shows high mobility of 2.45×10^{-1} cm^2/Vs that is about 100 times greater than that of the TiOPc single layer device, which originated from highly ordering, increasing of grain size and bigger channel conductance of TiOPc thin films deposited on a DH-α6T submonolayer.

References

[1] Law, K. Y. (1993). *Chem. Rev.*, *93*, 449.
[2] Mizuguchi, J., Rihs, G. G., & Karfunkel, H. R. (1995). *J. Phys. Chem.*, *99*, 16217.
[3] Bao, Z., Lovinger, A. J., & Dodabalapur, A. (1996). *Appl. Phys. Lett.*, *69*, 3066.
[4] Guillaud, G., Simon, J., & Germain, J. P. (1998). *Coord. Chem. Rev.*, *178–180*, 1433.
[5] Ye, R., Baba, M., Oishi, Y., Mori, K., & Suzuki, K. (2005). *Appl. Phys. Lett.*, *86*, 253505.
[6] Ye, R., Baba, M., & Mori, K. (2005). *Jpn. J. Appl. Phys.*, *44*, L581.
[7] Ye, R., Baba, M., Ohishi, Y., Mori, K., & Suzuki, K. (2006). *Mol. Cryst. Liq. Cryst.*, *444*, 203.
[8] Zeis, R., Siegrist, T., & Kloc, C. (2005). *Appl. Phys. Lett.*, *86*, 022103.
[9] Cornil, J., Calbert, J. P., & Brédas, J. L. (2001). *J. Am. Chem. Soc.*, *123*, 1250.
[10] Tada, H., Touda, H., Takada, M., & Matsushige, K. (2000). *Appl. Phys. Lett.*, *76*, 873.
[11] Saito, T., Sisk, W., Kobayashi, T., Suzuki, S., & Iwayanagi, T. (1993). *J. Phys. Chem.*, *97*, 8026.
[12] Brinkmann, M., Wittmann, J. C., Barthel, M., Hanack, M., & Chaumont, C. (2002). *Chem. Mater.*, *14*, 904.
[13] Yamashita, A., Maruno, T., & Hayashi, T. (1993). *J. Phys. Chem.*, *97*, 4567.
[14] Norton, J. E., & Bredas, J. L. (2008). *J. Chem. Phys.*, *128*, 034701.
[15] Li, L., Tang, Q., Li, H., Yang, X., Hu, W., Song, Y., Shuai, Z., Xu, W., Liu, Y., & Zhu, D. (2007). *Adv. Mater.*, *19*, 2613.
[16] Yonehara, H., Etori, H., & Pac, C. (2002). *Langmuir*, *18*, 7557.
[17] Loi, M. A., da Como, E., Dinelli, F., Murgia, M., Zamboni, R., Biscarini, F., & Muccini, M. (2005). *Nature Materials*, *4*, 81–85.
[18] Garnier, F., Yassar, A., Hajlaoui, R., Horowitz, G., Deloffre, F., Servet, B., Ries, S., & Alnot, P. (1993). *J. Am. Chem. Soc.*, *115*, 8716.
[19] Dinelli, F., Murgia, M., Levy, P., Cavallni, M., & Biscarini, F. (2004). *Phys. Rev. Lett.*, *92*, 116802.
[20] Yang, J., Wang, T., Wang, H., Zhu, F., Li, G., & Yan, D. (2008). *J. Phys. Chem. B*, *112*, 7816.
[21] Yang, J., Wang, T., Wang, H., Zhu, F., Li, G., & Yan, D. (2008). *J. Phys. Chem. B*, *112*, 7821.
[22] Yan, D., Wang, H., & Du, B. (2010). *Introduction to Organic Semiconductor Heterojunctions*, John Wiley & Sons: Singapore.
[23] Sze, S. M. (1981). *Physics of Semiconductor Devices*, Wiley, New York.
[24] Torsi, L., Marinelli, F., Angione, M. D., Dell'Aquila, A., Cioffi, N., De Giglio, E., & Sabbatini, L. (2009). *Organ. Electron.*, *10*, 233.